

Absence of a boron isotope effect in the magnetic penetration depth of MgB_2 D. DiCastro,¹ M. Angst,¹ D. G. Eshchenko,^{1,2} R. Khasanov,^{1,2} J. Roos,¹ I. M. Savic,³ A. Shengelaya,¹ S. L. Bud'ko,⁴ P. C. Canfield,⁴ K. Conder,⁵ J. Karpinski,⁶ S. M. Kazakov,⁶ R. A. Ribeiro,⁴ and H. Keller¹¹Physik-Institut der Universität Zurich, CH-8057 Zurich, Switzerland²Paul Scherrer Institute, CH-5232 Villigen PSI, Switzerland³Faculty of Physics, University of Belgrade, 11001 Belgrade, Yugoslavia⁴Ames Laboratory and Department of Physics and Astronomy, Iowa State University, Ames, IA 50011, USA⁵Laboratory for Neutron Scattering, ETH Zurich and PSI Villigen, CH-5232 Villigen PSI⁶Solid State Physics Laboratory, ETH, CH-8093 Zurich, Switzerland

The magnetic penetration depth $\lambda(0)$ in polycrystalline MgB_2 for different boron isotopes ($^{10}\text{B}/^{11}\text{B}$) was investigated by transverse field muon spin rotation. No boron isotope effect on the penetration depth $\lambda(0)$ was found within experimental error: $\lambda(0) = \lambda(0) = 0.8(8)\%$, suggesting that MgB_2 is an adiabatic superconductor. This is in contrast to the substantial oxygen isotope effect on $\lambda(0)$ observed in cuprate high-temperature superconductors.

PACS numbers: 74.70.Ad, 76.75.+i, 82.20.Tr, 71.38.-k

Since the discovery of superconductivity with transition temperature $T_c \approx 39\text{K}$ in the binary intermetallic compound MgB_2 [1], a large number of experimental and theoretical investigations were performed in order to explain the mechanism and the origin of its remarkably high transition temperature. Experiments were done revealing the important role played by the lattice excitations in this material [2, 3, 4, 5]. In particular, the substitution of the ^{11}B with ^{10}B has been demonstrated to shift T_c to higher temperatures [2, 3], as expected for a phonon mediated pairing mechanism.

However, MgB_2 differs from conventional superconductors in several important aspects, including, for instance, the unusually high T_c and the anomalous specific heat [6]. Calculations [7, 8] based on the Eliashberg formalism support the experimental results [6, 9, 10], revealing MgB_2 to be a two-band superconductor with two superconducting gaps of different size, the larger one originating from a 2D π -band and the smaller one from a 3D σ -band. The electronic π -states are confined to the boron planes and couple very strongly to the in-plane vibration of the boron atoms (E_{2g} phonon mode). This strong pairing, confined only to parts of the Fermi surface, is the principal contribution responsible for superconductivity and mainly determines T_c . The σ -states on the remaining parts of the Fermi surface form much weaker pairs. The double-gap structure explains most of the unusual physical properties of MgB_2 , such as the high critical temperature, the total T_c isotope-effect coefficient (≈ 0.32 [3]), the temperature dependent specific heat [6], tunneling [9] and upper critical field anisotropy $H_{c2}^{\text{ab}}/H_{c2}^{\text{c}}$ [11].

An interesting point to be clarified concerns the nature of the electron-lattice coupling. It was proposed [12, 13] that MgB_2 is a non-adiabatic superconductor. Alexandrov [12] suggested that, because of the large coupling strength of the electrons to the E_{2g} phonon mode, the many-electron system is unstable and breaks down into a

small polaron system, similar to the cuprate high temperature superconductors (HTSC), where the charge carriers are trapped by local lattice distortions. Cappelluti et al. [13] proposed that the small value of the Fermi energy E_F of the π -bands relative to the phonon energy $\hbar\omega_{\text{ph}}$ violates the adiabatic assumption ($\hbar\omega_{\text{ph}} \ll E_F$), opening up a non-adiabatic channel that enhances T_c . These models are in contrast to the conventional theory of superconductivity (Migdal adiabatic approximation), in which the density of states at the Fermi level, the electron-phonon coupling constant, and the effective supercarrier mass are all independent of the mass M of the lattice atoms. Both non-adiabatic models explicitly predict in MgB_2 a boron isotope effect (BIE) on the charge carrier effective mass m^* [12, 13]. Similar models [14, 15] were already used to explain the large oxygen isotope effect (OIE) on m^* observed in HTSC [16, 17, 18, 19, 20, 21] by measuring the OIE on the magnetic field penetration depth λ , a physical quantity directly related to the charge carrier effective mass.

In this letter, a muon spin rotation (SR) study of the magnetic penetration depth $\lambda(0)$ in polycrystalline MgB_2 for different boron isotopes ($^{10}\text{B}/^{11}\text{B}$) is reported. SR is a powerful microscopic tool to measure the magnetic penetration depth [22]. Indeed, in a polycrystalline type II superconductor with a perfect vortex lattice (VL) the average magnetic penetration depth can be extracted from the muon-spin depolarization rate $(T)/T^2(T)$ [22]. In our measurement, no BIE on $\lambda(0)$ was observed within experimental error [$\lambda(0) = \lambda(0) = 0.8(8)\%$], in contrast to the substantial OIE observed in cuprate HTSC [16, 17, 18, 19, 20, 21]. Our results imply that polaronic or non-adiabatic effects in MgB_2 are absent or negligibly small.

The SR experiments were performed on two polycrystalline MgB_2 samples containing ^{11}B (Mg^{11}B_2) and ^{10}B (Mg^{10}B_2). Full details of the sample synthesis are given in Refs [2, 23]. In brief, the two samples were synthe-

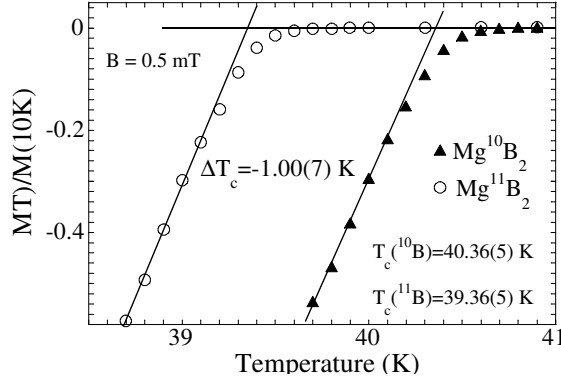


FIG. 1: Normalized field-cooled (0.5 mT) magnetization as a function of temperature for Mg^{10}B_2 and Mg^{11}B_2 samples.

sized using elemental Mg (99.9% pure in lump form) and isotopically pure boron (99.95% chemical purity, 99.5% isotope purity, < 100 mesh) combined in a sealed Ta tube in a stoichiometric ratio. The Ta tube was then sealed in a quartz ampoule, placed in a 950 °C box furnace for 24 hours, and then removed and allowed to cool to room temperature.

To examine the quality of the samples low field (0.5 mT, field-cooled) magnetization measurements were performed using a commercial Superconducting Quantum Interference Device. Figure 1 shows the temperature dependence of the magnetization for the Mg^{11}B_2 and Mg^{10}B_2 samples in the vicinity of T_c . The high quality of the two samples is revealed by the sharp transition and the high T_c extracted from the intercept of the linear extrapolations (Fig. 1): $T_c(^{10}\text{B}) = 40.36(5) \text{ K}$, $T_c(^{11}\text{B}) = 39.36(5) \text{ K}$. There is a clear isotope shift of $T_c = T_c(^{11}\text{B}) - T_c(^{10}\text{B}) = 1.00(7) \text{ K}$. The corresponding isotope effect coefficient $\beta = \frac{1}{T_c} \frac{dT_c}{d \ln(M_B)} = 0.29(2)$ (enrichment corrected) is in good agreement with previous results [2, 3].

The transverse-field SR experiments were performed at the Paul Scherrer Institute (PSI), Switzerland, using the M3 SR facility. The samples used for the magnetization measurements (see Fig. 1) were pressed in disk-shaped pellets with 10 mm diameter and 3 mm thickness and cooled in an external magnetic field B_{ext} perpendicular to the muon spin polarization from well above T_c to temperatures lower than T_c . The measurements were taken in a field of $B_{\text{ext}} = 0.6 \text{ T}$ (the highest available at PSI), high enough to avoid pinning induced distortion of the VL [24, 25, 26]. As shown in Fig. 2 for Mg^{11}B_2 at two different temperatures, the local magnetic field distribution can be very well approximated by a single Gaussian, centered at a field lower than the external one. This again indicates the high quality of the samples and the absence of any normal conducting domains. From the width of the Gaussian field distribution, which is propor-

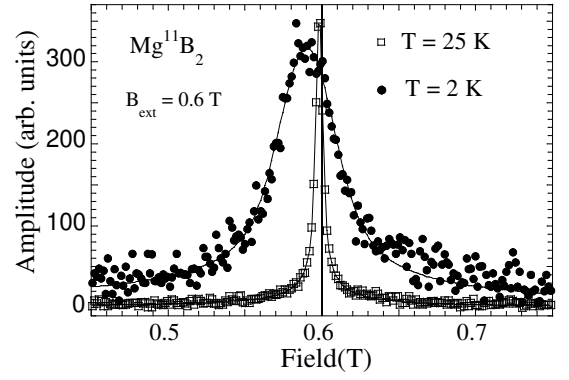


FIG. 2: Local magnetic field distribution, obtained from the Fourier transform of the muon spin precession signal, for Mg^{11}B_2 at 2 K (●) and 25 K (□). Solid lines are Gaussian fits to the experimental data. The vertical solid line indicates the external field of 0.6 T.

tional to the muon spin depolarization rate λ , the penetration depth λ_L , that is the length scale of the variation of the magnetic field, can be extracted using the relation $\lambda_L^2 = \lambda / \mu_0$.

In Fig. 3, the temperature dependence of λ_L for the Mg^{11}B_2 (●) and Mg^{10}B_2 (▲) samples is shown. Below T_c , λ_L for both samples starts to increase and saturates at low temperatures $T < 6 \text{ K}$, in agreement with previous SR measurements [25]. The data for the two samples close to T_c show a clear isotope shift of $T_c = 1.2(2) \text{ K}$, in agreement with T_c deduced from the low field magnetization measurements (Fig. 1). With decreasing temperature, the values of λ_L for the Mg^{11}B_2 sample are systematically lower than those for the Mg^{10}B_2 sample. However, at low temperature they merge together, indicating that there is no substantial BIE on $\lambda_L(0)$.

In order to quantify this observation, we performed fits to the experimental data. It was suggested [25, 26] that for the two-gap superconductor MgB_2 , the temperature dependence of λ_L can be written in the form:

$$\lambda_L(T) = \lambda_L(0) \left[w + (1-w) \frac{f(\xi_1/T)}{f(\xi_2/T)} \right] \quad (1)$$

with $\xi_i(T) = \frac{2 \cdot (0)}{k_B T} R_1 f(\xi_i/T) [1 - f(\xi_i/T)] d$.

Here, ξ_1 and ξ_2 are the zero temperature large and small gap, respectively, w is the relative contribution of the large gap to $\lambda_L(0)$, and $f(\xi_i/T)$ is the Fermi distribution. For the temperature dependence of the gaps we used the conventional BCS $\xi_i(T)$. In order to improve the ratio of the number of data point vs the number of fit parameters, the two gaps and w were considered as common fitting parameters for the two isotope data. As shown by the solid and dotted lines in Fig. 3, the experimental data are well described by Eq. (1). The fit yields: $\lambda_L(0)^{11\text{B}} = 9.79(10) \text{ s}^{-1}$, $\lambda_L(0)^{10\text{B}} = 9.95(11) \text{ s}^{-1}$, $w = 0.88(2)$, $\xi_1 = 4.9(1)$ and $\xi_2 = 1.1(3)$. All these values

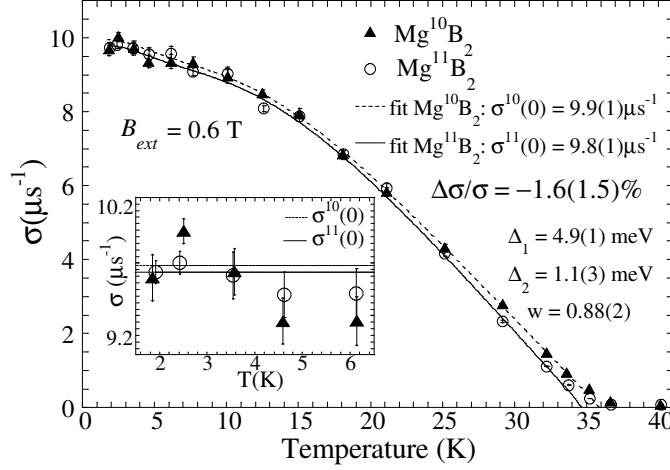


FIG. 3: Temperature dependence of σ at $B_{\text{ext}} = 0.6 \text{ T}$ for the two isotope samples Mg^{10}B_2 (\blacktriangle) and Mg^{11}B_2 (\circ). The solid (Mg^{10}B_2) and dotted (Mg^{11}B_2) lines are fits using Eq. (1). Inset: low-temperature region on a larger scale. The dotted and solid horizontal lines represent the weighed average values of $\sigma(0)$ for $T < 7.5 \text{ K}$ for Mg^{10}B_2 and Mg^{11}B_2 , respectively.

are in very good agreement with previous SR measurements performed by us on a natural boron MgB_2 sample and by Ohishi et al. [26]. It is interesting to note that the high value of w implies that only a very small contribution to $\sigma(0)$ originates from the γ -band, in accordance with the experimental finding that the superfluid density in the γ -band is strongly suppressed by an external magnetic field [6, 9].

The relative isotope shift of $\sigma(0)$ is: $(\sigma^{11}\text{B}/\sigma^{10}\text{B}) = (\sigma^{11}\text{B})/(\sigma^{10}\text{B}) = \sigma^{11}(0)/\sigma^{10}(0) = 0.98(8)\%$, corresponding to:

$$\sigma^{11}(0) = \sigma^{10}(0) = 0.98(8)\% : \quad (2)$$

For comparison, we calculated the relative isotope shift using a different and model independent procedure, taking the weighed average of the experimental points for $T < 7.5 \text{ K}$ (see inset of Fig. 3), where $\sigma(T)$ saturates. We obtained $\sigma^{11}(0)/\sigma^{10}(0) = 0.98(8)\%$. Both results are compatible with zero BIE on the penetration depth $\sigma(0)$.

Here, it is very important to recall that the two isotope samples used in the experiment were made with the same starting Mg for both the samples, and with ^{10}B and ^{11}B powders of the same mesh size (distribution of grain sizes), and were synthesized under exactly the same conditions. Therefore, we can exclude any influence on due to different grain size and to a difference in pinning or vortex dynamical effects.

To check the reliability of our results, a second measurement on a set (set B) of samples from different source and preparation technique and with smaller Meissner fraction, was performed in a field of 0.4 T . The results are very similar to the first set (set A) shown above:

$\sigma^{11}(0)/\sigma^{10}(0) = 0.98(8)\%$ as compared to the above $1.6(1.5)\%$. This shows that our result is intrinsic for MgB_2 and holds for lower fields as well. A summary of the results for both sets of isotope samples is given in Table I. Note that the values of $\sigma^{11}\text{B}$ and $\sigma^{10}\text{B}$ for set B measured in lower fields are larger than the corresponding values for set A. This is consistent with previous work [25, 26].

Theoretically, the zero temperature penetration depth is proportional to a density-of-states weighed average of a tensor involving the Fermi velocities. Detailed calculations within different formalisms have been carried out for MgB_2 (see Refs. [27, 28]). For our purpose it is sufficient to use the simpler London approach considering a free electron model and linking $\sigma(0)$ to the superconducting charge carrier density n_s and effective mass m , only considering different contributions from the γ and the σ bands. There is of course a direct connection between the Fermi velocities and the effective mass (a band average), both of which are not bare quantities, but in general renormalized, e.g., due to coupling with the phonons. The London approach has the advantage

TABLE I: Summary of the BIE results for $\sigma(0)$ obtained from the SR measurements of two sets of isotope samples.

	$\sigma^{10}\text{B}$ (μs^{-1})	$\sigma^{11}\text{B}$ (μs^{-1})	$\sigma^{11}(0)/\sigma^{10}(0)$	
Set A	9.95(11)	9.79(10)	0.016(15) ^a	0.005(8) ^b
Set B	12.91(17)	12.69(13)	0.015(17) ^a	0.016(30) ^b

^a from fit using Eq. (1)

^b from low temperature average (inset Fig. 3)

of facilitating the comparison with theoretical predictions [12, 13] and results obtained on cuprate superconductors [16, 17, 18, 19, 20, 21], all of which are formulated within this approach.

Unlike the cuprate superconductors with their extremely short coherence lengths, MgB_2 cannot be considered as being in the superclean limit and we need to consider a possible impact of scattering. In a moderately clean superconductor the penetration depth is related to the effective mass m^* by the following relation [29]:

$$\lambda = \frac{c}{v_F} = \frac{c}{\hbar k_F} = \frac{c}{\hbar} \frac{m}{n_s} \quad (3)$$

where n_s and m are the superconducting charge carrier density and effective mass, respectively, λ is the coherence length, and v_F is the mean free path. As already mentioned, the λ contribution (90%) to λ^2 in our experimental conditions comes from the σ -band. Therefore n_s , m , λ , and v_F in Eq.(3) have to be considered as σ -band values. It was estimated [30, 31] that in the σ -band ($m^* = 1.5$), a value which is close to the clean limit ($m^* = 1$). Therefore Eq. (3) may be approximated by $\lambda = \frac{c}{v_F} = \frac{c}{\hbar k_F} = \frac{c}{\hbar} \frac{m}{n_s}$. A shift in $\lambda = \frac{c}{v_F}$ due to the isotope substitution is then given by

$$\frac{\lambda^2(0)}{\lambda^2(0)} = \frac{n_s}{n_s} \frac{m}{m} : \quad (4)$$

The contribution from the supercarrier density n_s is negligible, as was already experimentally demonstrated in the case of HTSC [17, 18, 19, 21]. Specifically, for MgB_2 , it can be argued that: i) by changing the isotope only the mass of the nuclei is changed and not the charge carrier density n . Furthermore, MgB_2 is a stoichiometric compound; ii) x-ray diffraction measurements, performed on the samples used for the SR experiments, showed no substantial difference between the lattice parameters of $Mg^{11}B_2$ and $Mg^{10}B_2$. This implies that the band structure is not appreciably modified by the isotope substitution. Therefore, assuming $n_s = n_s = 0$ in Eq.(4) and neglecting the small σ -band contribution, we can estimate the boron isotope effect on the σ -band effective mass:

$$\frac{m^*}{m^*} = \frac{\lambda^2(0)}{\lambda^2(0)} = 1.6(1.5) \% : \quad (5)$$

Here we have used the value of the relative shift on $\lambda^2(0)$ obtained from the fit to Eq. (1). There is no BIE on the σ -band effective mass within experimental error.

Our result then suggests that non-adiabatic or polaronic effects in MgB_2 are absent or negligibly small, and establishes an upper limit [Eq. (2) and Eq. (5)] to any theoretical prediction of such effects [12, 13]. This conclusion is in contrast to cuprate superconductors, where a substantial oxygen isotope effect on m^* was observed [16, 17, 18, 19, 20, 21]. Recent magnetization measurements on MgB_2 under pressure [32] show no pressure effect on the magnetic penetration depth at low temperature, further supporting the main conclusion of the present work.

In summary, SR experiments on polycrystalline $Mg^{10}B_2$ and $Mg^{11}B_2$ samples revealed no substantial boron isotope effect on the magnetic penetration depth at $T = 0$ K. From this finding we conclude that there is no substantial BIE on the effective mass of the charge carriers in the σ -band. This result suggests that MgB_2 is a conventional phonon mediated superconductor without non-adiabatic or polaronic effects, in contrast to cuprate superconductors.

This work was partly performed at the Swiss Muon Source (S μ S) at the Paul Scherrer Institute (Villigen, Switzerland). We thank D. Herlach and A. Amato for technical assistance during the SR experiments at the Paul Scherrer Institute and T. Schneider for useful discussions. This work was supported by the Swiss National Science Foundation and by the NCCR Program MAEP sponsored by the Swiss National Science Foundation. Ames Lab is operated for the U.S. Department of Energy by Iowa State University under Contract No. W-7405-Eng-82. The work at the Ames Lab was supported by the Director of Energy Research, Office of Basic Energy Sciences.

Email: dicastro@physik.unizh.ch

- [1] J. Nagamatsu et al, Nature (London) 410, 63 (2001).
- [2] S. L. Bud'ko et al, Phys. Rev. Lett. 86, 1877 (2001).
- [3] D. G. Hinks, H. Claus, and J. D. Jorgensen, Nature 411, 457 (2001).
- [4] D. Di Castro et al, Europhys. Lett. 58, 278 (2002)
- [5] A. F. Goncharov and V. V. Struzhkin, Physica C 385, 117 (2003).
- [6] F. Bouquet et al, Phys. Rev. Lett. 87, 047001 (2001).
- [7] A. Y. Liu, I. I. Mazin, and J. Kortus, Phys. Rev. Lett. 87, 087005 (2001).
- [8] H. J. Choi et al, Nature 418, 758 (2002).
- [9] P. Szabo et al, Phys. Rev. Lett. 87, 137005 (2001).
- [10] S. Souma et al, Nature 423, 65 (2003).
- [11] M. Angst et al, Phys. Rev. Lett. 88, 167004 (2002).
- [12] A. S. Alexandrov, Physica C 363, 231 (2001).
- [13] E. Cappelluti et al, Phys. Rev. Lett. 88, 117003 (2002).
- [14] A. S. Alexandrov and N. F. Mott, Int. J. Mod. Phys. 8, 2075 (1994).
- [15] C. Grimaldi, E. Cappelluti, and L. Pietronero, Europhys. Lett. 42, 667 (1998).
- [16] G. M. Zhao and D. E. Morris, Phys. Rev. B 51, 16487 (1995).
- [17] G. M. Zhao et al, Nature (London) 385, 236 (1997).
- [18] G. M. Zhao, K. Conder, H. Keller, and K. A. Muller, J. Phys.: Condens. Matter 10, 9055 (1998).
- [19] J. Hofer et al, Phys. Rev. Lett. 84, 4192 (2000).
- [20] R. Khasanov et al, J. Phys.: Condens. Matter 15, L17 (2003).
- [21] R. Khasanov et al, cond-mat/0305477.
- [22] B. P. P. et al, Phys. Rev. B 42, 8019 (1990).
- [23] R. A. Ribeiro, S. L. Bud'ko, C. Petrovic, and P. C. Canfield, Physica C 385, 16 (2003).
- [24] Random flux pinning near the lower critical field H_{c1} may

induce distortion of the VL, giving rise to a field dependent χ which affects the value of χ .

- [25] Ch. Niedermayer et al, Phys. Rev. B 65, 094512 (2002)
- [26] K. Ohishi et al, J. Phys. Soc. Jpn. 72, 29 (2003)
- [27] V. G. Kogan, Phys. Rev. B 66, 020509 (2002).
- [28] A. A. Golubov et al, Phys. Rev. B 66, 054524 (2002).
- [29] M. Tinkham, Introduction to Superconductivity, Krieger Publishing Company, Malabar, Florida (1975).
- [30] A. V. Sologubenko et al, Phys. Rev. B 66, 014504 (2002).
- [31] F. Bouquet et al, Phys. Rev. Lett. 89, 257001 (2002).
- [32] D. Di Castro et al, unpublished.